Domain wall energy in quasi-one-dimensional Fe/W(110) nanostripes

M. Pratzer and H. J. Elmers
Institut für Physik, Johannes Gutenberg-Universität Mainz, Staudingerweg 7, D-55099 Mainz, Germany
(Received 4 July 2002; revised manuscript received 19 December 2002; published 21 March 2003)

The magnetic susceptibility in Fe/W(110) nanostripes decreases exponentially with increasing temperature according to an Arrhenius law which indicates a quasi-one-dimensional behavior. The interface energy of the Arrhenius law corresponds to the domain wall energy of a domain wall across a single stripe, separating fluctuating regions of homogeneous magnetization. The domain wall energy increases linearly with the width of the stripes, revealing a negative offset which we attribute to boundary effects. Domain wall energies have been determined for Fe/W(110) nanostripes coated with Au and Pd and are compared to values for uncoated Fe/W(110) nanostripes in ultrahigh vacuum.

DOI: 10.1103/PhysRevB.67.094416 PACS number(s): 75.75.+a, 75.70.Ak, 75.30.Cr

I. INTRODUCTION

The change of magnetic properties caused by spatial restrictions in the nanometer regime is an active research topic.[1] Magnetic properties will undergo a transition from three-dimensional ''bulk'' behavior to a quasi-two-dimensional behavior if one dimension is spatially restricted.[2–5] In addition, physical properties are dominated by deviating interface properties, i.e., interface anisotropies.[5] The case of spatial restriction in one dimension heavily gained from improved preparation techniques, revealing new phenomena, i.e., indirect exchange coupling.[6–8] A restriction in two dimensions, leading to a quasi-one-dimensional system, will win further understanding of the physics of magnetic nanostructures which is crucial for future electronic devices that work on a nanometer scale. Most promising for the preparation of quasi-one-dimensional systems is the deposition of parallel stripes at step edges of vicinal single crystal surfaces.[9] This method was used to prepare magnetic Fe island chains on Cu(111)[10] and ultrathin Fe films on stepped W(110),[11] revealing hints on quasi-one-dimensional magnetic properties. Continuous magnetic Fe/W(110) nanostripes, the one-dimensional analogon to three-dimensional bulk and two-dimensional ultrathin films, reveal the significance of dipolar coupling for perpendicular[12,13] and in-plane magnetization.[14] Recently, monoatomic Co chains, the closest approach to a one-dimensional system, could be prepared on vicinal Pt(111).[15,16]

Due to strong in-plane anisotropies,[17] the easy axis in the pseudomorphic monolayer Fe(110)/W(110) is along $[1\bar{1}0]$. The extremely strong uniaxial anisotropy is responsible for the two-dimensional (2D) Ising-like phase transition[18] in extended UHV/Fe/W(110) monolayers and for atomic-scale magnetic domain walls in stripes.[19] Smooth monolayer stripes can be grown only along [100]-oriented steps.[14] Accordingly, the easy axis in those stripes is in-plane, but perpendicular to the stripe axis, resulting in substantial dipolar coupling between adjacent stripes. As was pointed out in Ref. 14, ferromagnetic order in the monolayer stripe system is triggered by this dipolar coupling (dipolar superferromagnetism), in contrast to the extended monolayer, where magnetic order results from exchange coupling, only. Within a stripe full width spin blocks of homogeneous magnetization are preformed by the exchange interaction at temperatures close to the dipolar induced magnetic phase transition of the stripe array. The dipolar coupling between spin blocks in adjacent stripes freezes the fluctuation of the spin blocks at a finite temperature, in contrast to the expected behavior of a single stripe. In addition to the ferromagnetic dipolar coupling a weak antiferromagnetic lateral indirect exchange coupling between adjacent stripes was found for Au coated stripes.[20]

For temperatures well above the Curie temperature a magnetic coupling between the stripes can be neglected[20] and a quasi-one-dimensional (1D) behavior predicted by theory[21] could be observed experimentally for Fe stripes grown on vicinal Cu(111)[10] and on vicinal W(110).[19] In this article we exploit the temperature dependence of the magnetic susceptibility above the Curie temperature to evaluate domain wall energies separating fluctuating antiparallel spin blocks for Au/Fe/W(110) and Pd/Fe/W(110) stripes. A comparison with previously determined values for UHV/Fe/W(110) stripes[19] shows a strong reduction of the domain wall energies indicating reduced anisotropies in the coated systems.

II. EXPERIMENTAL DETAILS

Experiments have been performed in UHV. Fe was grown by molecular beam deposition on single crystalline W(110) surfaces following previously described precedures.[22] The base pressure of the UHV apparatus was below 1×10^{-10} Torr and increased during deposition to 5×10^{-10} Torr. The deposited Fe films were characterized structurally and chemically using low energy electron diffraction (LEED), Auger spectroscopy (AES), and scanning tunneling microscopy (STM).[22,19] We took advantage of a W(110) crystal with a surface consisting of two polished planes: a well oriented surface ($\pm0.1°$ from [110]) and a surface where the surface normal deviates from [110] by $1.4°\pm0.1°$, resulting in atomic steps along the in-plane [001] direction with a mean step separation of 9.1 ± 0.6 nm. The terrace width corresponds to $W_0=41$ atomic rows. On the well oriented surface terraces are considerably wider (50 nm–150 nm) with a broad distribution and irregular orientation. Fe grows pseudomorphically on the W(110) surface and forms stripes attached to the step edges after annealing at 700

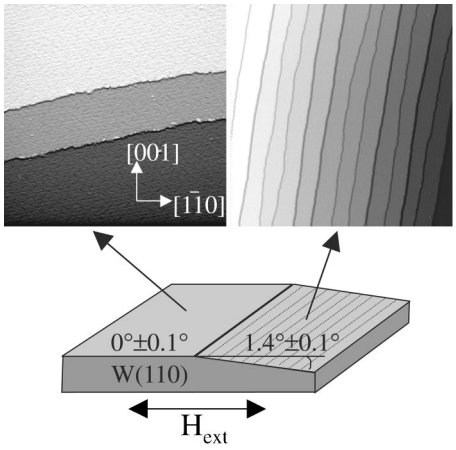

FIG. 1. Schematic drawing of the substrate crystal and STM images (200 nm×200 nm) from the flat and vicinal surface of the substrate.

K. For a coverage Θ, the mean width W of the Fe stripes is given by $W=W_0\Theta$. On the stepped surface the deposited iron forms an array of parallel nanostripes of monolayer height and a width of a few nanometers. We observe a distribution of widths with a full width at half maximum of $\Delta W/W=0.3$.[14,22] We measured magnetic properties directly after preparation and after covering the stripes at room temperature by 6 monolayers of Au and Pd. Previous Mössbauer studies confirmed that at room temperature Fe/Au interdiffusion does not occur.[23] Figure 1 shows schematically the sample geometry.

Magnetic properties werde studied by Kerr magnetometry. Using a compensation technique, we measured the Kerr ellipticity ϵ_K or the Kerr roation θ_K in absolute units, as a function of external field and temperature. In the following, we assume that Kerr angles are proportional to the magnetization M with respect to temperature and field dependence. The magnetic easy axis in the monolayer Fe/W(110) shows along $[1\bar{1}0]$; the anisotropies are comparatively large [4 meV/atom (Ref. 19)]. The external field was applied along the easy axis, i.e., perpendicular to the long stripe axis. Magnetization loops were measured during slowly warming up with a rate of about 1 K/min, after cooling with liquid nitrogen down to 100 K. One loop was measured in 2 min, thus limiting the temperature resolution to 2 K. In order to study properties as a function of coverage, we prepared wedge shaped samples with a slope of 1 ML/4 mm in addition to samples of homogeneous coverage.

III. RESULTS

A. Saturation and remanent magnetization

As an example we show magnetization loops of 0.7 ML Fe on vicinal W(110), corresponding to a stripe width of 28 AR (atomic rows), and coated by Au, in Fig. 2. At the lowest temperature ($T=111$ K) we observe a typical easy axis loop resulting from a switching between two stable magnetization states at the coercive force of $\mu_0 H=30$ mT. The remanent signal equals the signal at saturation. The loop confirms that

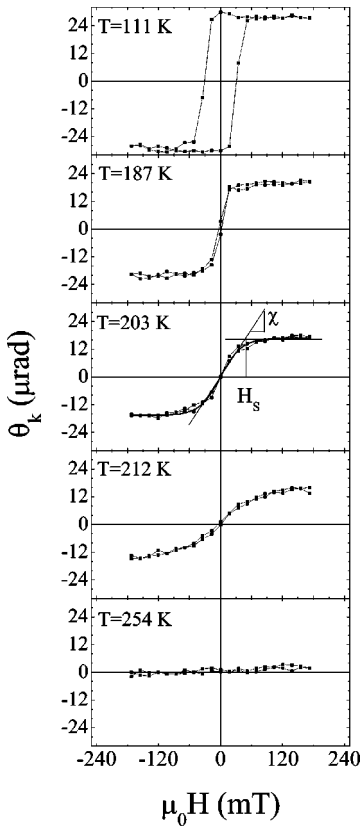

FIG. 2. Magnetization loops measured for Au/Fe/W(110) stripes with a mean stripe width $W=28$. With increasing temperature a transition from easy axis loops to magnetization curves following a tanh function, shown examplarily for $T=203$ K (full line), is observed.

the easy axis lies along $[1\bar{1}0]$. At $T=187$ K the remanence is almost zero. For higher temperatures the magnetization loops can be fitted by $\theta_K/\theta_{K,s}=\tanh(H/H_s)$ with the two parameters: saturation value $\theta_{K,s}$ and saturation field H_s. For a wide temperature range $\Delta T/T_C\approx 1$, H_s appears to be smaller than our maximum available field, in contrast to the typical bulk behavior.

Values for $\theta_{K,s}$ and for the remanence $\theta_{K,r}$ as derived from the magnetization loops are plotted in Fig. 3(c) and 3(e). for Au and Pd covered stripes, and in Fig. 3(d) and 3(f) for Au and Pd covered monolayers. Data from previous experiments on uncoated Fe nanostripes and monolayers are shown for comparison [Figs. 3(a) and 3(b)]. In the following, we denote the temperature of vanishing remanence as the Curie temperature $T_C(\Theta)$, which depends on the coverage Θ. The flat bare monolayer undergoes a two-dimensional Ising-like phase transition with no strong domain-induced paramagnetic response above T_C, whereas the flat covered monolayers show a saturation value of the magnetic signal up to 50 K above T_C. The temperature interval between T_C and the disappearance of the saturation signal is even larger for stripes on the terraced surface and occurs moreover in the case of bare stripes, too. For the case of bare stripes, this behavior was explained by a dipolar-induced phase transition.[14] A key point to distinguish remanence induced

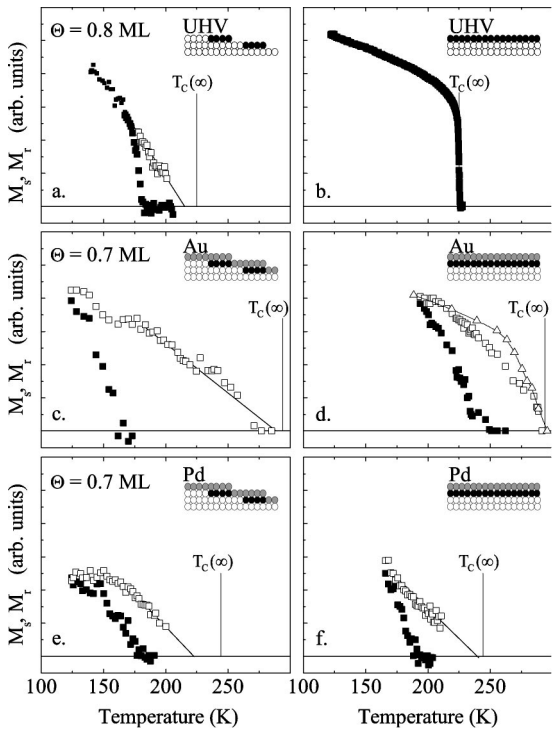

FIG. 3. Saturation (open symbols) and remanent (full symbols) values of magnetic signal versus temperature, for Fe(110)/W(110) monolayer stripes (left column) and extended monolayers (right column), uncovered (first line), covered by Au (second line), or Pd (third line), respectively. (a) Saturation (open squares) and remanent (full squares) Kerr ellipticity (data from Ref. 24). The linear extrapolation (thin line) of $M_s(T)$ indicates the critical temperature T_s as obtained from $M_s(T_s)=0$. (b) Remanent magnetization signal measured by spin-polarized low energy electron diffraction (Data from Ref. 25). (c)–(f) Saturation (open squares) and remanent (full squares) Kerr rotation. Data for the magnetic hyperfine field $B_{hf}(T)$ (open triangles) (Ref. 23). normalized to the Kerr ellipticity at the lowest temperature, is shown in (d). The Curie temperature $T_C(\infty)=T_s(\Theta\rightarrow 1)$ of an ideal, infinitely large two-dimensional Fe/W(110) monolayer (see Fig. 4) is indicated for comparison.

dipolar coupling from remanence induced by a lower relaxation time is the sharp transition width of $\Delta T_C=2$ K. For uncoupled stripes the distribution of stripe widths observed by STM would result in a Gaussian distribution of critical temperatures $\Delta T_C=15$ K. Convolution of this distribution of T_C values with the temperature dependence of remanence following a power law would result in a phase transition width smeared out over 40% of the mean value of T_C,[14] i.e., over 70 K. The difference between the temperature where remanence deviates from saturation and T_C is smaller for all systems discussed here and we assume that the phase transition is of the dipolar induced type. Moreover, for the case of bare and Au coated stripes we excluded relaxation of the remanence by measuring the remanent signal at different times after the field was switched off.

Au covered Fe monolayers on well oriented W(110) surfaces were measured previously by Mössbauer spectroscopy,[23] resulting in a Curie temperature close to room temperature in contradiction to the data presented here. The data for the magnetic hyperfine field $B_{hf}(T)$, normalized to the Kerr values at the lowest temperature, is shown for comparison [Fig. 3(d)]. The temperature dependence of $B_{hf}(T)$ rather follows the saturation value $\theta_{K,s}(T)$ than the remanence. Note, that Mössbauer spectroscopy is not sensitive to the direction of magnetization and the transition time is about 0.1μs; i.e., if the magnetization does not change during this transition time but shows arbitrarily parallel or antiparallel to a given easy axis, the measured hyperfine field will be the same as for a stable homogeneously magnetized sample. Only Mössbauer transitions at atoms where a magnetization switch occurs during the transition time create a paramagnetic component with $B_{hf}=0$. An additional paramagnetic component was indeed observed in the Mössbauer experiment for $T>200$ K. Fluctuating spin blocks with comparatively long time intervals between flips thus explain the contradictory statements for the Curie temperature of the Au/Fe/W(110) monolayer.

From this picture it follows that the observed small saturation fields (in a significant temperature range above T_C) compared to paramagnetic systems are due to the fact that the spin blocks behave as a single giant moment. In contrast to a superparamagnetic system the single moment is temperature dependent as a consequence of the temperature dependend length of a spin block. When the system is saturated at small fields (<0.2 T), all spin blocks are magnetized in the same direction and the measured saturation signal corresponds to the mean magnetization within a spin block. The magnetization within a spin block will be smaller than the ground state magnetization because of fluctuating single spins within the spin block (preferably at the boundaries), which can only be aligned in fields which are orders of magnitude larger. The magnetization within a spin block will vanish at a temperature where the thermal energy equals the exchange energy, which is the case at the Curie temperature $T_C(\infty)$ of a stripe of infinite width, i.e., a (hypothetical) two-dimensional system. Therefore we tentatively extrapolate the saturation signal $M_s(T)$ linearly to $M_s(T_s)=0$, as indicated in Fig. 3. This extrapolation defines a temperature T_s, which will be smaller than $T_C(\infty)$ for narrow stripes but T_s approaches $T_C(\infty)$ for wide stripes grown on the flat surface.

Figure 4 shows T_C and T_s as a function of the Fe coverage. T_C and T_s is higher for films grown on the flat surface than for stripes on the vicinal surface. Both values T_C and T_s increase with increasing Fe coverage. The steplike increase of T_C and T_s observed for Au covered nanostripes [Fig. 4(a)] below the coverage $\Theta=1$ indicates the occurrence of antiferromagnetic lateral indirect exchange coupling as discussed in Ref. 20. For submonolayers grown on the flat surface T_s approaches a saturation value for Fe coverages close to the full monolayer [Figs. 4(b) and 4(d)]. For the following, we assume that this saturation value of T_s, measured on the flat surface, equals the Curie temperature of the infinitely large monolayer $T_C(\infty)$. The temperature interval between T_C and T_s denotes the temperature regime of fluctuating spin blocks. For $T>T_s$ the single spins fluctuate independently from each other, and saturation fields will become large according to the Curie-Weiss law. One should note, that the transition from the spin block to the paramagnetic tempera-

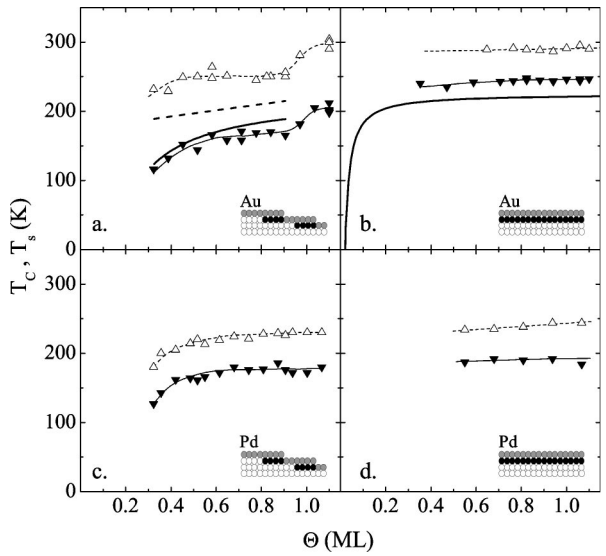

FIG. 4. Curie temperature T_C (full triangles) and critical temperature T_s (open triangles) versus coverage Θ for parallel stripes grown on the vicinal surface and covered by (a) Au and (c) Pd. Thin full and dotted lines are a guides to the eye. In (b) and (d) similar data are shown for extended monolayers grown on the flat W(110) surface. Thick lines represent data for uncovered UHV/Fe/W(110) stripes taken from Refs. 14,24 and for uncovered UHV/Fe/W(110) monolayer films taken from Ref. 25.

ture regime is a gradual transition. T_s does not mark a critical phase transition. If infinitely large external fields were available, H_s would continue to increase through and above T_s. The determination of T_s is related to the use of a comparatively small field. Our assumption $T_s(\Theta \rightarrow 1) = T_C(\infty)$ is justified for UHV/Fe/W(110) monolayers on the flat surface, because the magnetic phase transition is close to a two-dimensional Ising system[18] and T_C almost equals T_s. It is justified in the case of Au/Fe/W(110) monolayers, because Mössbauer spectroscopy[23] revealed a Curie temperature similar to our value $T_s(\Theta \rightarrow 1)$. For Pd/Fe/W(110) monolayers we tentatively use the same assumption.

B. Susceptibility

We now focus on the temperature region $T_C < T < T_s$ analyzing the temperature dependence of the magnetic susceptibility. We model the magnetic susceptibility of a single stripe consisting of W parallel rows of spins by an Ising model.[26] The short range interaction involved in the Ising model is accompanied by long range dipolar interaction and the applicability of the model will be discussed below. For a one-dimensional Ising model the magnetic susceptibility is given by $\chi \propto (1/T)\exp(2J/k_B T)$. For the case of stripes the exchange coupling constant J is replaced by WJ.[26,27,21] If the stripe width W is finite, no spontaneous order will occur according to the one-dimensional Ising model. For $T < T_s$ the magnetization decomposes into fluctuating spinblocks of full stripe width and a length L increasing with decreasing temperature.[26] These full width spin blocks act similar as the moments of an Ising chain. The magnetization decays exponentially at any finite temperature and no remanent order is left. The quasi one-dimensional behavior shows up in the exponential decrease of the magnetic susceptibility with increasing temperature T:[27]

$$\chi_0 = \frac{C}{T}\exp\left(\frac{k_B T_A}{k_B T}\right), \tag{1}$$

where T_A denotes the energy of an interface beween two spin blocks. In the case of the Ising model T_A corresponds to $2JW$. T_A will be lower if one considers finite anisotropies. C depends weakly on the temperature because single fluctuating spins decrease the average magnetic moment within a spin block.

An additional dipolar coupling between adjacent stripes in a stripe array will modify the susceptibility. The long range nature of the coupling (reduction of $1/r^2$ instead of exponential decrease with distance r) justifies a mean field ansatz and we obtain the susceptibility of the stripe array[20]

$$\chi = \frac{\chi_0}{1 - \chi_0 \lambda}, \tag{2}$$

with the mean field constant λ. The lateral coupling thus provokes a diverging susceptibility for $\chi_0(T_C) = 1/\lambda$ indicating the onset of spontaneous order at a finite temperature T_C. Equation (2) can be approximated in two different temperature regions. For $T \gg T_C$ the coupling can be neglected since χ_0 decreases rapidly with increasing temperature, i.e., $\chi = \chi_0$. This approximation was exploited to determine the domain wall energy in Ref. 19 of bare stripes. For T close to T_C, however, Eq. (2) can be linearized ($1/\chi \propto T - T_C$). This behavior was confirmed for bare Fe stripes,[14] too. The boundary between these temperature regimes is given by[20] $T_b = T_C T_A/(T_A - T_C)$.

Susceptibility data for Fe coverages below the full monolayer are presented in the Arrhenius plots shown in Fig. 5 according to Eq. 1. For all three investigated systems we observe a linear behavior. The susceptibility deviates systematically from the Curie-Weiss law. Obviously, the data cannot be described by a power law, in contrast to three- and two-dimensional systems. The linear behavior observed for this plot agrees with the one-dimensional behavior according to Eq. (1), neglecting the dipolar coupling between adjacent stripes. An interstripe coupling would increase χ above the value for uncoupled stripes for T close to T_C [Eq. (2)]. Oppositely, finite size effects tend to decrease χ, thus supressing the divergence at T_C. In our experiment the linear behavior extends almost down to $T = T_C$. This striking observation might be attributed to a compensation of finite size effects and dipolar coupling.

In the following analysis we neglect the dipolar coupling between adjacent stripes, which is strictly valid only for $T \gg T_b$, and approximate the susceptibility data by Eq. 1. We also have to consider a dipolar coupling along an individual stripe (intrastripe dipolar coupling). The intrastripe dipolar coupling is smaller than the inter-stripe dipolar coupling. Therefore we assume that this contribution can be neglected, too. Note, that the fit with Eq. (1) instead of Eq. (2) might overestimate T_A to some extent. For Pd covered stripes the

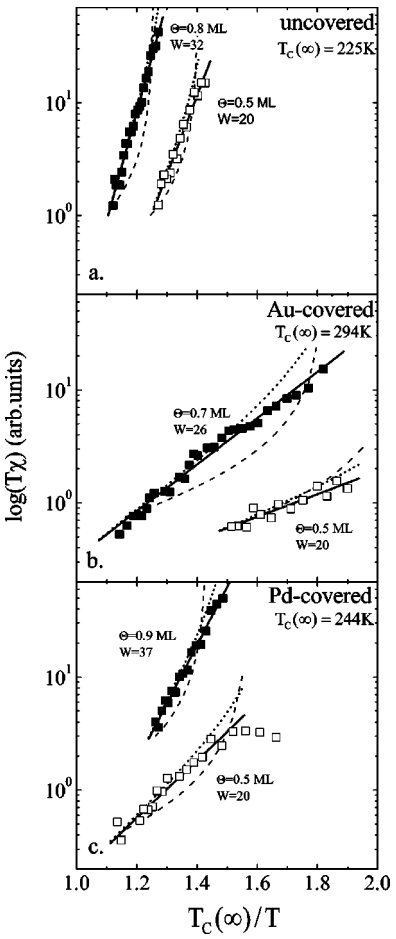

FIG. 5. Temperature dependence of the normalized magnetic susceptibility $\ln(T\chi)$ versus reciprocal temperature $T_C(\infty)/T$. (a) UHV/Fe/W(110) stripes (data from Ref. 19), (b) Au/Fe/W(110) stripes, and (c) Pd/Fe/W(110) stripes. The linear behavior (drawn line) confirms the exponential temperature dependence of χ (Arrhenius law). For Au and Pd coated stripes the slope, corresponding to the interface energy T_A, is considerably smaller than in the case of uncoated stripes. For comparison, Curie-Weiss laws (dashed lines) and expected data when dipolar coupling is considered [Eq. (2), dashed line] using the appropriate value for T_C are shown.

temperature range of useful data is particularly small and the analysis as a one-dimensional system must be considered with some care.

Figure 6 shows values for T_A as determined for coverages $\Theta = 0 - 1.1$ ML, corresponding to stripe widths $W = 0 - 45$ AR. Below a stripe width of 35 AR we observe a linear increase of T_A with increasing stripe width for the case of Au-coated and Pd-coated stripes. We fit the data for $W < 35$ AR with the linear approximation

$$k_B T_A = \epsilon_W W - e_b . \tag{3}$$

Data for uncoated stripes increase with increasing stripe width, too, however the experimental error is larger. Data from the fits are summarized in Table I. Deviations from the linear increase observed for $W > 35$ indicate a morphological change. If the stripe width approaches the full coverage of

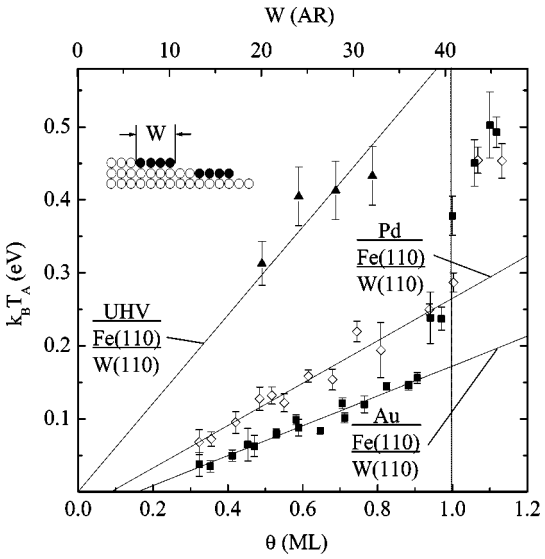

FIG. 6. Interface energy $k_B T_A$ as determined from Arrhenius plots versus stripe width $W = \Theta W_0$, $W_0 = 41$. Data taken from wedge shaped samples Au/Fe/W(110), Pd/Fe/W(110) and from a series of homogenously prepared UHV/Fe/W(110) samples. Solid lines indicate linear fits. For UHV/Fe/W(110) stripes the axial section was set to zero.

the terraces the stripes will overlap. In this case the susceptibility deviates from the Arrhenius law and values for T_A as determined from the mean slope in the Arrhenius plot cannot be interpreted as a domain wall energy.[19]

IV. DISCUSSION

In the simplest approximation one would expect T_A to be proportional to the width of the stripes, as has been assumed in Ref. 19. In the case of Au- and Pd-covered stripes we observe an offset value $e_b \approx 30$ meV, instead. This observation can be interpreted as a boundary correction resulting from the stripe edges. Because T_A was determined in the temperature region $T_C < T < T_s$, i.e., above the magnetic phase transition, the results can be compared to Monte Carlo

TABLE I. Curie temperature $T_C(\infty)$ of an ideal, infinitely large two-dimensional Fe/W(110) monolayer as extrapolated from extended Fe/W(110) monolayers grown on the flat W(110) surface. Specific domain wall energy ϵ_W per atomic row and boundary correction e_b for Fe stripes as determined from the linear approximation $T_A(W)$. Values for the exchange integral J were calculated from the two-dimensional Ising relation $k_B T_C(\infty) = 2.26J$. Anisotropy energy per atom e_K resulting from the micromagnetic model for continuous matter (Bloch wall), $\epsilon_W = 2\sqrt{Je_K}$.

X/Fe/W(110)	X=UHV	X=Au	X=Pd
$T_C(\infty)$ (K)	225±10	294±5	244±10
ϵ_W (meV)	15.2±1.5	5.0±0.3	7.2±0.6
e_b (meV)		32±7	27±14
J (meV)	8.6±0.3	11.2±0.2	9.3±0.4
e_K (meV)	6.7±1.6	0.6±0.1	1.4±0.3

(MC) simulations for the Ising model of single monolayer stripes. Similar boundary corrections have been observed in these MC simulations.[26] In the simulation the temperature dependence of the magnetization relaxation time follows the exponential law $\tau \propto \exp[T_{A,\tau}(W)/T]$.[26] A linear increase of $T_{A,\tau}(W)/T_C(\infty) = pW - q$ with constants $p = 3.13$ and $q = 3.31$ was obtained,[26] suggesting that a half circle domain wall of radius W circumferences the critical nucleus for a new spin block and a boundary correction q must be considered.[14] An analogous boundary correction can be expected for the correlation length and the magnetic susceptibility, respectively, however with different constants p and q. For an Ising system the constant for the linear increase p was shown to be $p = 0.884$ in agreement with $k_B T_A(W) = 2JW$ ($J = 0.884 k_B T_C(\infty)/2$ being the exchange integral).[26,21] A boundary correction q for the susceptibility was not determined by MC simulations. Our experimental result for the boundary correction suggests a value of $q = e_B/k_B T_C(\infty) \approx 1$ that is independent of the specific domain wall constant p which might deviate from its Ising value due to finite anisotropies.

The specific domain wall energy ϵ_W can be related to the exchange stiffness A and to the anisotropy constant K (Ref. 19) of the uniaxial anisotropy. Assuming that the domain wall can be modeled by the classical continuum micromagnetic model,[28] i.e., minimizing the functional $\int [A(\phi'(x))^2 + K \sin^2\phi(x)]dx$, the domain wall energy per area for the simplest case of a Bloch wall is given by $\sigma_W = 4\sqrt{AK}$. For a Néel wall K has to be replaced by $K + J_s^2/2\mu_0$, corresponding to a correction of 0.36 meV/atom.[28] For a comparison with theoretical data, exchange stiffness and anisotropy can be expressed in the atomic measures, exchange integral J and anisotropy per atom e_K as follows: Starting from localized magnetic moments at the lattice sites of the Fe atoms, the Hamiltonian for an anisotropic Heisenberg model is given by

$$H = -J \sum_{\langle i,j \rangle} s_i s_j - e_K \sum_i \cos^2 \theta_i , \tag{4}$$

with spin operator s_i and θ_i specifying the angle between s_i and the easy axis. In the following we set $|s_i| = 1$, i.e., the value of J includes the spin quantum number S^2. Only nearest neighbor interaction is considered (summation over $\langle i,j \rangle$). For simplification we consider $s_i s_j$ being a scalar product of classical vectors and with the lattice constant of tungsten $a = 0.316$ nm we obtain $K = 2e_K/a^3$ and $A = cJ/(2a)$.[29] Note, that here the assumption $s_i s_j \approx 1$ is crucial. The structure dependent constant $c = 1$ equals the value for the simple cubic case because of the missing nearest neighbors in the bcc(110) monolayer.

In the case of the pseudomorphic Fe/W(110) monolayer the area S_{DW} of the domain wall is given by $S_{\mathrm{DW}} = W(a/\sqrt{2})^2$ and we obtain $\sigma_W = 2\epsilon_W/a^2$ and consequently, $\epsilon_W = 2\sqrt{Je_K}$ and the domain wall width $w = 2\sqrt{A/K} = a\sqrt{J/e_K}$. Using the experimental information of the domain wall width measured by high resolution spin-polarized scanning tunneling microscopy for UHV/Fe/W(110) stripes, constants A and K were determined independently from each other.[19] From the experimental values of $\epsilon_W = e_W/W = 15.2$ meV and $w = 0.6$ nm an exchange integral $J = 14$ meV and an effective anisotropy $e_K = 4$ meV per atom was obtained.[30] A boundary correction was neglected in this case, i.e., $e_B = 0$. It should be noted that a boundary correction of the order of $e_B = 30$ meV would not change ϵ_W within its error limits. For wall widths of only $1-2$ lattice constants the continuum model might be questionable and the values given in Refs. 19,30 can be seen as an upper limit. An evaluation of the same experimental data using a model of localized spin results in $e_K = 3.6$ meV.[31] From *ab initio* calculations a value of $e_K = 2.3$ meV was reported[32] for the case of a magnetization rotation from $[1\bar{1}0]$ to $[001]$. Anisotropy constants of the UHV/Fe/W(110) monolayer have not been measured by magnetometry, yet. However, an extrapolation from thicker films was given in Ref. 33: $e_K = 0.6$ meV, which is obviously too small. The exchange integral can be estimated from $T_C(\infty) = 225$ K for the extended UHV/Fe/W(110) monolayer: The magnetic phase transition of this system can be well described by the 2D-Ising model.[18] For the 2D-Ising model the Curie temperature is related to J by $k_B T_C(\infty) = 2.26J$;[34] hence we obtain $J = 8.6$ meV in fair agreement with the experimentally determined value.

For the Au- and Pd-covered case no data for the domain wall width is available. In order to determine the anisotropy we estimate the exchange integral from $T_C(\infty)$ measured for extended Fe monolayers grown on the flat area of the tungsten substrate. Whereas J turns out to be approximately 10 meV in all three cases, the Au and Pd coverage reduces ϵ_W considerably and the anisotropy e_K by an order of magnitude due to the quadratic dependence. For a Ag covered monolayer an out-of-plane anisotropy of $e_K = 0.4$ meV was measured by magnetometry[35] in agreement with the value obtained for the Au covered case. As a further consequence of the reduced anisotropy, the domain wall width is expected to be increased for the Au- and Pd-covered case. Hence, the micromagnetic model is even better justified.

The thermodynamical behavior of stripes undergoes a transition from quasi-one-dimensional behavior to a two-dimensional behavior with increasing stripe width. For UHV/Fe/W(110) stripes the transition occurs between $W = 32$ and the mean terrace width on the well oriented W(110) substrate, $W_0 \approx 200$ as determined by STM. The crucial parameter which determines the critical width for this transition is the ratio e_K/J. If the ratio is small, i.e., $e_K/J \ll 1$, as in the case of Au/Fe/W(110), the critical width increases and the influence of lateral restrictions become more dominant even for wide stripes. We observed indeed an exponential temperature dependence of the magnetic susceptibility even for the Au/Fe/W(110) monolayer on the well oriented surface of the substrate. From T_A we could extrapolate a nominal stripe width of $W = 150$ using the linear dependence $T_A(W)$ described above, which fits nicely to the mean terrace width of the flat substrate. This observation indicates that for the Au covered case the maximum available terrace width, limited by the mosaic spread of the tungsten single crystal, is too small to allow for the observation of a two-dimensional magnetic phase transition. This also explains the critical exponents $\beta \approx 1/3$,[23] which strongly deviate from the expected

2D-Ising value 1/8. Contrarily, from the theoretical point of view a comparatively small uniaxial anisotropy is sufficient to provoke a two-dimensional Ising behavior.[36]

V. CONCLUSION

In conclusion we have shown that Fe nanostripe arrays grown on stepped W(110) and covered by Pd and Au show a quasi one dimensional thermodynamic behavior. The magnetic susceptibility decreases exponentially with increasing temperature following an Arrhenius law. The interface energy in the Arrhenius law can be interpreted as a domain wall energy. The interface energy increases linearly with the stripe width. In the case of Au/Fe/W(110) and Pd/Fe/W(110) stripes we observed a common boundary correction for the interface energy. The interface energy for Au- and Pd-covered stripes is strongly reduced in comparison to stripes with a free surface. Assuming that the exchange integral does not significantly depend on the coverage material, this means that the anisotropy energy is reduced—because of the quadratic dependence—by an order of magnitude for the case of covered stripes. Previously not understood temperature dependencies of the magnetic hyperfine field for Fe/W(110) monolayers can be explained by a finite step density which is present even on well oriented substrate surfaces in combination with the small anisotropies.

ACKNOWLEDGMENTS

We thank J. Hauschild for handing over previously unpublished data. H.J.E. thanks U. Gradmann for fruitful discussions and for careful reading of the manuscript. This work was supported by the Deutsche Forschungsgemeinschaft.

[1] J. Shen, J. Kirschner, Surf. Sci. **500**, 300 (2002).
[2] S. D. Bader, Surf. Sci. **500**, 172 (2002).
[3] *Ultrathin Magnetic Structures* edited by J.A.C. Bland and B. Heinrich (Springer Verlag, Berlin, 1992), Vols. I, II.
[4] H. J. Elmers, Int. J. Mod. Phys. B **9**, 3115 (1995).
[5] U. Gradmann, in *Handbook of Magnetic Materials*, edited by K. H. J. Buschow (Elsevier, Amsterdam, 1993), Vol. 7.
[6] P. Grünberg, R. Schreiber, Y. Pang, M.B. Brodsky, and H. Sowers, Phys. Rev. Lett. **57**, 2442 (1986).
[7] M. N. Baibich, J. M. Broto, A. Fert, F. Nguyen Van Dau, F. Petroff, P. Etienne, G. Creuzet, A. Friederich, and J. Chazelas, Phys. Rev. Lett. **61**, 2472 (1988).
[8] S. S. P. Parkin, N. More, and K. P. Roche, Phys. Rev. Lett. **64**, 2304 (1990).
[9] F. J. Himpsel, J. E. Ortega, G. K. Mankey, and R. F. Willis, Adv. Phys. **47**, 511 (1998).
[10] J. Shen, R. Skomski, M. Klaua, H. Jenniches, S. S. Manoharan, and J. Kirschner, Phys. Rev. B **56**, 2340 (1997).
[11] J.-S. Suen and J. L. Erskine, Phys. Rev. Lett. **78**, 3567 (1997).
[12] H.J. Elmers, J. Hauschild, and U. Gradmann, Phys. Rev. B **59**, 3688 (1999).
[13] J. Hauschild, U. Gradmann, and H.J. Elmers, Appl. Phys. Lett. **72**, 3211 (1998).
[14] J. Hauschild, H. J. Elmers, and U. Gradmann, Phys. Rev. B **57**, R677 (1998).
[15] P. Gambardella, A. Dallmeyer, K. Maiti, M. C. Malagoli, W. Eberhardt, K. Kern, and C. Carbone, Nature (London) **416**, 301 (2002).
[16] A. Dallmeyer, C. Carbone, W. Eberhardt, C. Pampuch, O. Rader, W. Gudat, P. Gambardella, and K. Kern, Phys. Rev. B **61**, R5133 (2000).
[17] U. Gradmann, J. Korecki, and G. Waller, Appl. Phys. A: Mater. Sci. Process. **39**, 101 (1986).
[18] H. J. Elmers, J. Hauschild, and U. Gradmann, Phys. Rev. B **54**, 15 224 (1996).
[19] M. Pratzer, H. J. Elmers, M. Bode, O. Pietzsch, A. Kubetzka, and R. Wiesendanger, Phys. Rev. Lett. **87**, 127201 (2001).
[20] M. Pratzer and H. J. Elmers, Phys. Rev. B **66**, 033402 (2002).
[21] E. V. Albano, K. Binder, D. W. Heermann, and W. Paul, Z. Phys. B: Condens. Matter **77**, 445 (1989).
[22] H. J. Elmers, J. Hauschild, and U. Gradmann, J. Magn. Magn. Mater. **221**, 219 (2000).
[23] U. Gradmann, G. Liu, H. J. Elmers, and M. Przybylski, Hyperfine Interact. **57**, 1845 (1990).
[24] H. Hauschild, Ph.D. thesis, TU Clausthal, 1998.
[25] H. J. Elmers, J. Hauschild, H. Höche, U. Gradmann, H. Bethge, D. Heuer, and U. Köhler, Phys. Rev. Lett. **73**, 898 (1994).
[26] P. Sen, D. Stauffer, and U. Gradmann, Physica A **245**, 361 (1997).
[27] M. Müller and W. Paul, J. Stat. Phys. **73**, 209 (1993).
[28] A. Hubert and R. Schäfer, *Magnetic Domains* (Springer, Berlin, 1998).
[29] S. Chikazumi, *Physics of Ferromagnetism* (Oxford Science, Oxford, 1997).
[30] In Ref. 19 $k_B T_A$ was erroneously set as $2e_W$ whereas the correct relation is $k_B T_A = e_W$. As a consequence, correct values for exchange stiffness A and anisotropy constant K are $A = 3.6^{+2.2}_{-1.4} \times 10^{-12}$ J/m and $K = 40.6^{+26}_{-15} \times 10^6$ J/m^3.
[31] M. Lippert, H. J. Elmers, and P. van Dongen (unpublished).
[32] X. Nie, G. Bihlmayer, and S. Blügel (unpublished).
[33] H. J. Elmers, J. Magn. Magn. Mater. **185**, 274 (1998).
[34] L. Onsager, Phys. Rev. **65**, 117 (1944).
[35] H. J. Elmers, G. Liu, and U. Gradmann, Phys. Rev. Lett. **63**, 566 (1989).
[36] M. Bander and D. L. Mills, Phys. Rev. B **38**, 12 015 (1988).